Activity and in vivo tracking of Amphotericin B loaded PLGA nanoparticles

ARTICLE *in* EUROPEAN JOURNAL OF MEDICINAL CHEMISTRY · MAY 2015

Impact Factor: 3.45 · DOI: 10.1016/j.ejmech.2015.03.022

21 AUTHORS, INCLUDING:

Ana Camila Oliveira Souza

University of São Paulo

7 PUBLICATIONS **27** CITATIONS

SEE PROFILE

Nathalia Moraes de Vasconcelos

Ghent University

3 PUBLICATIONS **32** CITATIONS

SEE PROFILE

Antonio Cláudio Tedesco

University of São Paulo

221 PUBLICATIONS **3,133** CITATIONS

SEE PROFILE

Anamelia L Bocca

University of Brasília

59 PUBLICATIONS **590** CITATIONS

SEE PROFILE

European Journal of Medicinal Chemistry 95 (2015) 267–276

Contents lists available at ScienceDirect

European Journal of Medicinal Chemistry

journal homepage: http://www.elsevier.com/locate/ejmech

Original article

Activity and *in vivo* tracking of Amphotericin B loaded PLGA nanoparticles

A.C.O. Souza [a, 1], A.L. Nascimento [a, 1], N.M. de Vasconcelos [a], M.S. Jerônimo [a], I.M. Siqueira [a], L. R-Santos [b], D.O.S. Cintra [a], L.L. Fuscaldi [c], O.R. Pires Júnior [a], R. Titze-de-Almeida [b], M.F. Borin [c], S.N. Báo [a], O.P. Martins [e], V.N. Cardoso [d], S.O. Fernandes [d], M.R. Mortari [a], A.C. Tedesco [e], A.C. Amaral [f, *], M.S.S. Felipe [a, g], A.L. Bocca [a]

[a] Biology Institute, University of Brasília, DF, Brazil
[b] Faculty of Agronomy and Veterinary Medicine, University of Brasília, DF, Brazil
[c] Biotechnology Department, Health Sciences Faculty, University of Brasília, DF, Brazil
[d] Pharmacy Department, Federal University of Minas Gerais, MG, Brazil
[e] Chemistry Department of FFCLRP, University of São Paulo, Ribeirão Preto, SP, Brazil
[f] Biotechnology, Institute of Tropical Pathology and Public Health, Federal University of Goiás, GO, Brazil
[g] Genomic Science and Biotechnology Post-Graduate Program, Catholic University of Brasília, DF, Brazil

ARTICLE INFO

Article history:
Received 13 October 2014
Received in revised form
11 March 2015
Accepted 12 March 2015
Available online 14 March 2015

Keywords:
Amphotericin B
PLGA nanoparticles
Biodistribution
Antifungal activity

ABSTRACT

The development of biocompatible polymeric nanoparticles has become an important strategy for optimizing the therapeutic efficacy of many classical drugs, as it may expand their activities, reduce their toxicity, increase their bioactivity and improve biodistribution. In this study, nanoparticles of Amphotericin B entrapped within poly (lactic-co-glycolic) acid and incorporated with dimercaptosuccinic acid (NANO-D-AMB) as a target molecule were evaluated for their physic-chemical characteristics, pharmacokinetics, biocompatibility and antifungal activity. We found high plasma concentrations of Amphotericin B upon treatment with NANO-D-AMB and a high uptake of nanoparticles in the lungs, liver and spleen. NANO-D-AMB exhibited antifungal efficacy against *Paracoccidioides brasiliensis* and induced much lower cytotoxicity levels compared to D-AMB formulation *in vivo* and *in vitro*. Together, these results confirm that NANO-D-AMB improves Amphotericin B delivery and suggest this delivery system as a potential alternative to the use of Amphotericin B sodium deoxycholate.

1. Introduction

Amphotericin B is a natural polyene antifungal commonly used in therapy against severe systemic fungal infections [1]. The administration of this drug is done by intravenous injection, which is quite inconvenient for long periods because of the need for continuous and prolonged venous access, in addition to the adverse effects and toxicity related to its use [1,2]. Severe adverse toxic side effects are associated with the use of Amphotericin B sodium deoxycholate (D-AMB), mainly renal failure. Alternative nanostructure-based formulations, such as lipid formulations and polymeric nanoparticles, have demonstrated antifungal efficacy and lower toxicity, decrease in the active principle dose and increase in the accessibility of the drug to organs and targeted tissue [1,3].

Lipid-based preparations for Amphotericin B, such as liposomal Amphotericin B (AMBISOME®) considerably reduced the toxicity

Abbreviations: D-AMB, Amphotericin B sodium deoxycholate; PLA, polylactic acid; PGA, poly glycolic acid; PLGA, poly (lactic-co-glycolic) acid; PBS, phosphate buffered saline; DMSA, dimercaptosuccinic acid; NANO-D-AMB, nanoparticles of Amphotericin B sodium deoxycholate entrapped in a poly (lactic-co-glycolic) acid and dimercaptosuccinic acid matrix; NANO-PLGA, nanoparticles of poly (lactic-co-glycolic) acid and dimercaptosuccinic acid without Amphotericin B; PI, polydispersity index; ZP, zeta potential; MTT, 3-(4-5-dimethylthiazol-2-yl)-2,5-diphenyl tetrazolium bromide; 99mTc-DMSA, Technetium-99m radiolabeled dimercaptosuccinic acid; 99mTc-NANO-D-AMB, poly (lactic-co-glycolic) acid nanoparticles containing Amphotericin B and Technetium-99m radiolabeled dimercaptosuccinic acid; PCM, paracocidioidomycosis.

* Corresponding author. Biotecnologia/Instituto de Patologia Tropical e Saúde Pública, Universidade Federal de Goias, Rua 235, S/N, Setor Universitario, Goiania, GO 74.060-050, Brazil.
E-mail address: amaral.nanobio@gmail.com (A.C. Amaral).
[1] These authors equally contributed to this work.

http://dx.doi.org/10.1016/j.ejmech.2015.03.022
0223-5234/

caused by this drug [4]. Recently, polymeric formulations composed of poly (lactic-co-glycolic) acid (PLGA) have also been proposed as a promising alternative to circumvent the adverse effects induced by treatment with this antifungal [5–10]. This strategy is also appropriate for target-delivery of the drug to specific organs in the body [3].

Previous data from our group [3] proposed a new formulation for D-AMB entrapped within PLGA and dimercaptosuccinic acid (DMSA) nanoparticles (NANO-D-AMB). It was demonstrated that NANO-D-AMB had the same antifungal effectiveness as D-AMB *in vivo*, with the advantage of being administered each three days (instead of daily), with sustained release of Amphotericin B and no increase in the toxic effects of the treatment, thus allowing a reduction in the number of injections [3].

NANO-D-AMB nanoparticles were evaluated *in vivo* against paracoccidioidomycosis (PCM), a systemic mycosis endemic to Latin America, characterized as a lung chronic granulomatous infection caused by the thermo-dimorphic fungus from *Paracoccidioides* genre [11]. D-AMB is the therapeutic option for the severe forms of PCM, and it is used as the first choice in intravenous therapy until the remission of the disease, in which the patient should be transferred to the maintenance phase with the use of oral drugs, such as trimetrophim-sulphametoxazol and azoles [12]. Since the infection is located mainly in the lungs, it was useful to evaluate the polymeric Amphotericin B formulation associated with dimercaptosuccinic acid, which has a preferential tropism to the lungs [13].

These previous results prompted questions about physic-chemical characteristics of the NANO-D-AMB nanoparticle and its biosafety and biodistribution. The present study reports the physic-chemical characterization of NANO-D-AMB and its biocompatibility *in vivo* and *in vitro*, apart from a comparison of antifungal effectiveness *in vivo* with D-AMB and AMBISOME®.

2. Material and methods

Amphotericin B sodium deoxycholate (Sigma, St Louis, MO, USA) containing 45% of pure Amphotericin B and 35% of sodium deoxycholate was used as treatment and to prepare nanoparticles. The polylactic acid (PLA), polyglycolic acid (PGA) and DMSA used to prepare the nanoparticles were also purchased from Sigma (St Louis, MO, USA). AMBISOME® (Gilead, USA), the liposomal formulation of Amphotericin B, was the therapeutic agent used to compare the *in vivo* antifungal activity, and Anforicin B® (Cristália, Brazil), a commercial D-AMB formulation, was used to compare the pharmacokinetic parameters.

BALB/c or Swiss mice aged 6–8 weeks obtained from the animal facility of the Faculty of Pharmaceutical Sciences of Ribeirão Preto (University of São Paulo, Brazil) were used for the *in vivo* toxicity and antifungal activity assays and in the pharmacokinetics assays. A total of 12 mice per experimental condition were used, and the experiments were repeated three times independently. Animals were housed under controlled light conditions and were provided with food and water *ad libitum*. All animal procedures performed in this study were approved by the Animal Care and Use Committee of the University of Brasília, Brasília DF, Brazil.

2.1. Nanoparticles preparation

PLGA nanoparticles containing Amphotericin B and dimercaptosuccinic acid (NANO-D-AMB) were prepared as previously described [3]. Briefly, 50 mg of PLA and 50 mg of PGA were first dissolved in dichloromethane. Then, an aqueous solution containing 1% of polyvinyl alcohol was added to the polymeric mixture to obtain the initial water-in-oil emulsification. To this solution it was added 120 mg of D-AMB with DMSA, and the mixture was submitted to vigorous agitation in a blender (10,000 rpm). The water-in-oil emulsification was also obtained by vigorous agitation in an ULTRA-TURRAX stirrer. The organic solvent was removed from the solution by stirring at room temperature and evaporation under reduced pressure. The nanoparticles were washed three times in distilled water (10 min, 25 °C, 5000 rpm), suspended in 1 mL of phosphate buffered saline (PBS) and stored at 4 °C. All procedures were performed in a sterile room with all the manipulation in a sterility hood. Nanoparticles prepared by the same described method without the addition of Amphotericin B (NANO-PLGA) were obtained and used as a control.

2.2. Zeta potential of the nanoparticles

Physicochemical characterization of nanocarriers was performed by their mean size, polydispersity index (PI), and zeta potential (ZP). The mean size and PI of colloidal dispersions were performed at 25 °C in the range 100–2000 Hz by laser light scattering and zeta potential was measured according to the particle's electrophoretic mobility using the equipment ZEN3600 Zetasizer Nano ZS (Malvern, UK). In both determinations (solutions of NANO-D-AMB or NANO-PLGA), samples were analyzed following appropriate dilution with filtered ultrapure water. Data are represented as the mean (±SD) of three different batches.

2.3. Morphology of the nanoparticles

Morphologic characteristics of the nanoparticles were accessed using transmission electron microscopy (TEM) and scanning electron microscopy (SEM). For TEM, aliquots of the nanoparticle solution were placed on a copper grid, previously coated with Formvar (0.7%) and dried at room temperature. The material was then observed in a transmission electron microscope (TEM, JEOL 1011, 80 kV) and images were captured using a Gatan Ultrascan camera. Under SEM, the nanoparticles were deposited on a support with a carbon strip after being fixed with 4% paraformaldehyde and washed with distilled water. The samples were coated with gold and analyzed in the equipment JEOL JSM-700.

2.4. Release profile of Amphotericin B from nanoparticles

To study the kinetic release of Amphotericin B from nanoparticles *in vitro*, a sample of NANO-D-AMB in PBS was diluted to 10 μg/ml and samples were incubated at 37 °C at 150 rpm for 2 h, 24 h, 48 h, and 72 h. For each time point, samples were centrifuged and the supernatant was evaluated for percentage of D-AMB released from nanoparticles using High Performance Liquid Chromatography (HPLC). Samples of D-AMB dissolved in PBS were processed by the same protocol described above and were used as controls. Each set of nanoparticles and controls were analyzed in triplicate.

2.5. High performance liquid chromatographic analysis

The samples were analyzed in HPLC System Shimadzu LC-10A equipped with photodiode array detector SPD MXA-10. Chromatographic conditions were: Shim-pack CLC-ODS column (6.0 × 150 mm, Shimadzu, Japan); mobile phase 10 mM EDTA (pH 4.65) in 60% Acetonitrile; 1.5 mL/min isocratic flow per 10 min; UV retention established in 382 nm. The identification was carried by comparison of chromatographic fraction with the Amphotericin B standard, observing the retention time in chromatography system and UV scan spectrograms similarity in 200–300 nm range.

2.6. In vitro toxicity

To investigate whether nanoparticles could have any toxic effect on red cells a hemolysis assay adapted from previous studies was performed [7,14]. Human blood was collected in EDTA treated tubes and red cells were isolated, distributed in 96-well plate and incubated for 6 h at 37 °C with distilled water, PBS, NANO-D-AMB or D-AMB in the final concentrations of 1.56–600 μg/mL. After incubation times, the absorbance of sample supernatants was measured on 540 nm.

The toxicity of the nanoparticles on mammalian cells was accessed by a viability assay with 3-(4-5-dimethylthiazol-2-yl)-2,5-diphenyl tetrazolium bromide (MTT). 5×10^5 viable peritoneal cells were distributed on a 96-well plate in RPMI media (supplemented with 2% of Fetal Bovine Serum) and incubated for 24 h at 37 °C and 5% of CO_2. After this period, culture supernatants were substituted by a medium solution containing the formulations with a corresponding concentration of 8 μg/mL of Amphotericin B. The MTT assay was performed after 24 h, 48 h, and 72 h of incubation, and absorbance of the resulting Formazan crystals diluted in DMSO was determined at 540 nm.

2.7. In vivo acute toxicity assay

To verify the possible acute toxicity caused by NANO-D-AMB and D-AMB, healthy mice received an intraperitoneal (ip) injection with 6 mg/kg/day (1×) or 30 mg/kg/day (5×) of Amphotericin B of both formulations. After three days, animals were euthanized and blood, peritoneal and bone marrow cells were collected. Levels of blood urea nitrogen (BUN), creatinine, pyruvic acid and pyruvic and oxaloacetic glutamic transaminases (GPT; GOT) were determined by colorimetric Jaffé method. Genotoxicity was evaluated by DNA fragmentation assessment through propidium iodide labeling of bone marrow cells and analysis by Flow Cytometry adapted as described previously [15,16]. Mice undergoing treatment with cyclophosphamide (Genuxal®, Baxter, Brazil) in a single dose of 40 mg/kg were euthanized on the day following treatment and used as a control for DNA fragmentation. Cyclophosphamide is a nitrogen mustard compound known as a human carcinogen, able to form DNA adducts, DNA cross-links, and single and double-strand DNA breaks in dividing cells. Finally, in order to assess whether intraperitoneal treatment with studied formulations could induce inflammatory cell recruitment, it was made a smear of peritoneal cells collected by 10 mL cold PBS washing. After staining with Giemsa & Wright hematologic dye, cells were visualized in a magnification of 1000× in oil-immersion, and the percentage of neutrophils, monocytes and lymphocytes was determined.

2.8. Pharmacokinetic investigation

To investigate the pharmacokinetic parameters of the NANO-D-AMB nanoparticles, Swiss mice were randomly arranged in groups of five individuals and received a single dose of NANO-D-AMB or Anforicin B® containing 6 mg/kg of Amphotericin B by intraperitoneal route. After 24 h, 48 h or 72 h of treatment, animals were anesthetized with ketamine 10% (100 mg/kg) and xylazine 2% (10 mg/kg) followed by euthanasia and samples of lungs and blood were collected and stored at −20 °C until the moment of analysis.

The collection of blood and lungs samples and tissue extraction of Amphotericin B and piroxicam were performed according to previous publications [17–24]. To the collected plasma it was added 200 μL of piroxicam at 2.5 mg/mL, as the HPLC internal standard. The lungs were collected and macerated with 500 μL of deionized water and 200 μL of piroxicam 2.5 mg/mL prepared in methanol. To all the samples of plasma and lungs it was added 500 μL of DMSO (to break the PLGA polymer and to solubilize D-AMB) and 1 mL of methanol for protein precipitation by HPLC. The tissue mixture was appropriately homogenized, transferred to the Bond Ellut SPE column. The assay was performed according to manufacture's instructions and then the samples were processed by HPLC.

2.9. Biodistribution investigation

To evaluate the *in vivo* biodistribution parameters of NANO-D-AMB we used radiolabeled DMSA to prepare the nanoparticles. Radiolabeled DMSA was made using a lyophilized kit containing 1 mg of DMSA and 0.4 mg of $SnCl_2.2H_2O$. This kit was radiolabeled with 370MBq (10 mCi) of Technetium-99m in 1 mL of saline for 10 min at room temperature. The radiolabeled DMSA (99mTc-DMSA) were incorporated within PLGA nanoparticles loaded with Amphotericin B obtaining thus the radiolabeled 99mTc-DMSA nanoparticles (99mTc-NANO-D-AMB). The free 99mTc-DMSA and 99mTc-NANO-D-AMB were injected intravenously in mice and after 1 h and 8 h animals were anesthetized and euthanized, and images of biodistribution were obtained on a gamma camera. Samples of blood, spleen, stomach, liver, lungs and kidneys were collected to determine the radioactivity counted in gamma radiation per gram of sample.

2.10. In vivo antifungal therapy

BALB/c mice were infected as described by Marques et al. [25] and then subjected to different treatment regimens. Briefly, virulent yeasts of *Paracoccidioides brasiliensis* (Pb18 isolate) were cultivated at 37 °C on Brain Heart Infusion (BHI) liquid medium, and after seven days, culture was washed twice in PBS and yeast viability was assessed by staining with 0.05% Green Janus [26]. Mice were anesthetized as described previously and 3×10^5 viable yeast cells in a 50 μL inoculum were injected by intratracheal route. The treatments with NANO-D-AMB at three different concentrations of Amphotericin B (3, 4.5, and 6 mg/kg) were compared with the treatment using 2 mg/kg of the micellar D-AMB formulation (which is the recommended dose for clinical treatment of this mycosis), all of which were initiated 30 days after infection and had a duration of 60 days. In a second approach, treatment with NANO-D-AMB or the liposomal formulation AMBISOME® was compared using the same corresponding dose of 6 mg/kg of Amphotericin B, initiated 60 days after infection and continuing for 30 days. Injections were performed by intraperitoneal route and were conducted once a day (D-AMB treated groups) or once every three days (treatments with NANO-D-AMB, AMBISOME® or PBS). Non-infected and mock-treated animals were used as controls. After the treatment period, mice were euthanized and biological samples were collected for further analysis. To access fungal burden, lung homogenates were plated on BHI agar supplemented with 4% horse serum, 5% *P. brasiliensis* 192 isolate culture filtrate supernatant and 40 mg/L gentamicin and after 21 days at 37 °C, Colony Forming Units (CFU) were counted. Lung homogenate supernatant was also used to quantify IL-10, TNF-α and IL-12 by ELISA. Lymphoproliferation capacity was accessed through spleenocyte culture in RPMI medium (supplemented with 2 mM of L-glutamine, 50 μM β-mercaptoethanol, 5% Fetal Bovine Serum, 1 mM Sodium Piruvate and 1% non-essential aminoacids) stimulated or not with 4 μg/mL of Concanavalin-A (Con-A, Sigma, USA) or protein extract of *P. brasiliensis* Pb18 isolate in a proportion of 1 μL per 500 μL (PE 1:500). After 48 h of incubation at 37 °C and 5% CO_2, samples were pulsed with 1μCi/well of tritiated thymidine, and thymidine incorporation was determined using a beta-scintillation counter liquid.

2.11. Statistical analysis

The results shown are representative of three different experiments. Graphs show the values of the replicates ± standard error of the mean (SEM). To determine differences between experimental groups, analysis of variance (ANOVA) was used followed by Bonferroni method (post-test) performed in GraphPad PRISM statistical software, version 5.0 (GraphPad Software, USA, 2007). Data were considered significant when $p < 0.05$, whereas $^{*}p < 0.05$, $^{**}p < 0.01$ and $^{***}p < 0.001$ versus control groups described in legends. The software PASW® Statistics version 17.0 was also used. The results of Amphotericin B pharmacokinetics were expressed as mean ± standard deviation and ANOVA followed by Tukey's test for comparisons. For results involving two groups, we used the unpaired *t* test and Mann–Whitney test.

3. Results

3.1. Physicochemical and morphological characterization

The TEM analysis of the nanoparticles demonstrated a uniform spherical shape, with a variation in size distribution, including both isolated and agglomerated particles (Fig. 1A–D). The SEM analysis of the nanoparticles (Fig. 1E–H) supported TEM data, evidencing a smooth nanoparticle surface and slight aggregation.

Average diameter (D), zeta potential (ZP) and polydispersity index (PI) of NANO-D-AMB and NANO-PLGA were measured by the range of time of 21 days and were summarize in Table 1.

Table 1
Measurements of average diameter (D), zeta potential (ZP) and polydispersity index (PI) of NANO-D-AMB and NANO-PLGA samples.

NANO-D-AMB	D (nm)	ZP (mV)	PI
Day 1	394.6 ± 3.0	−15.2 ± 0.9	0.260
Day 7	347.6 ± 2.0	−20.4 ± 1.6	0.239
Day 14	333.7 ± 3.0	−21.2 ± 2.2	0.253
Day 21	343.0 ± 2.0	−21.4 ± 1.8	0.258
NANO-PLGA	D (nm)	ZP (mV)	PI
Day 1	320.0 ± 1.0	−30.0 ± 0.2	0.230
Day 7	321.6 ± 2.0	−33.6 ± 1.0	0.233
Day 14	327.3 ± 3.0	−32.1 ± 1.1	0.222
Day 21	329.7 ± 2.0	−31.8 ± 1.0	0.229

Data are presented as mean (±SD) of three different batches.

3.2. In vitro release of Amphotericin B from nanoparticles

The release pattern of Amphotericin B from NANO-D-AMB was evaluated. An initial burst release of 30.5% was detected after 24 h of *in vitro* incubation and there was continued release of the drug over two days, 13.6 ± 0.9% and 15.0 ± 1.7%, respectively (Fig. 1H). A significant accumulative concentration of Amphotericin B was not observed during the 72 h analyzed because the absorbance decreased quickly in solution. This data corroborate with previous

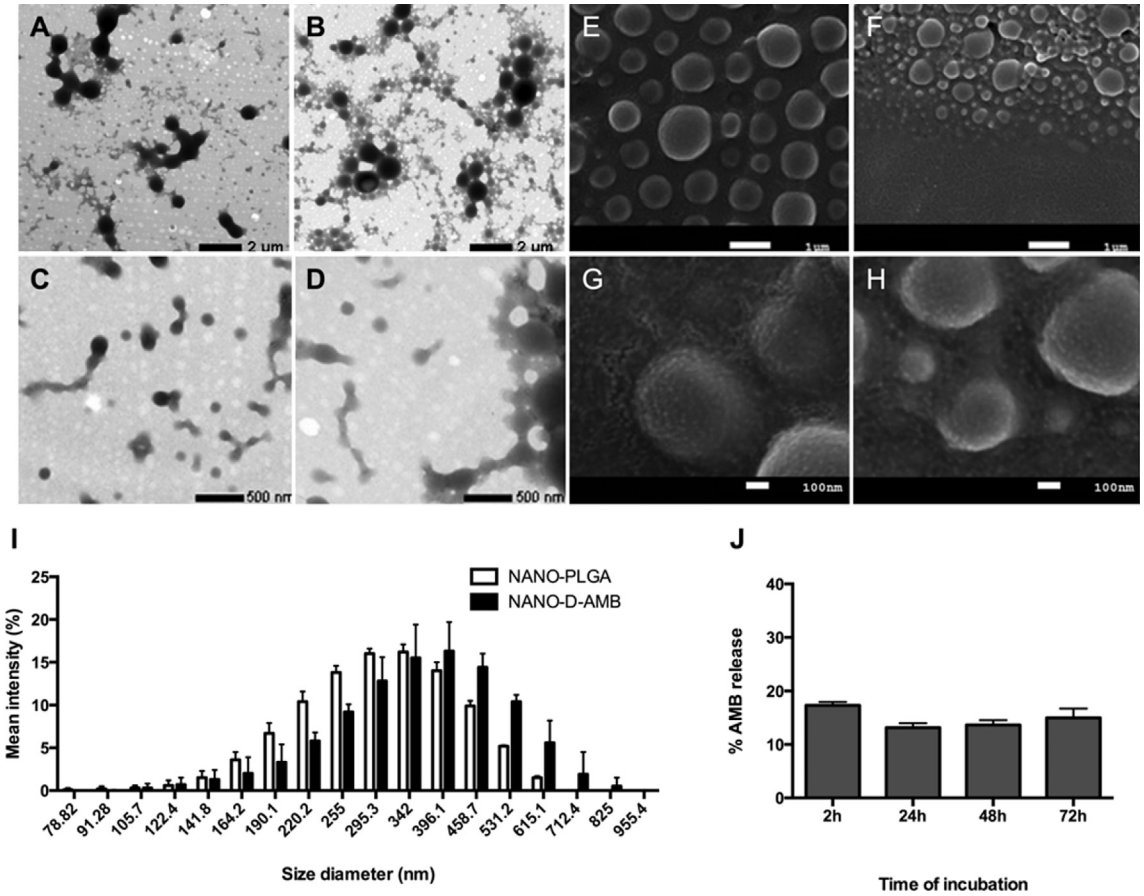

Fig. 1. Physiochemical and morphological characterization of NANO-D-AMB. TEM photomicrographs of NANO-PLGA (A, C) and NANO-D-AMB (B, D) nanoparticles at 10,000× (A, B) and 20,000× (C, D) magnification. SEM photomicrographs of NANO-PLGA (E, G) and NANO-D-AMB (F, H) nanoparticles at 8000× (E, F) and 45,000× (G, H) magnification. Histogram of size distribution of NANO-PLGA and NANO-D-AMB nanoparticles (I). Percentage of Amphotericin B release from NANO-D-AMB nanoparticles observed over 2, 24, 48 and 72 h of incubation in solution (J).

results that indicates inactivation of the drug in solution [27].

3.3. In vitro and in vivo safety of NANO-D-AMB

Thereafter, the biosafety of NANO-D-AMB was assessed. In the hemolytic assay with red blood cells, D-AMB formulation induced higher hemolysis levels, even in lower concentrations (Fig. 2A) while the other tested formulations were hemolytic only at very high concentrations. Besides that, D-AMB treatment caused a decrease in the viability of peritoneal macrophages after 24 h, 48 h, and 72 h of *in vitro* incubation at a concentration of 8 μg/mL of Amphotericin B (Fig. 2B), while viability levels for the other formulations were similar with those of mock-treated cells.

The *in vivo* analysis of genotoxicity in bone-marrow cells of healthy animals treated with a regular (1×) or an overdose (5×) of D-AMB, NANO-D-AMB and PBS demonstrated no significant differences in the amount of fragmented DNA between groups (Fig. 2C), while treatment with Cyclophosphamide, which causes DNA breaks in dividing cells, induced high levels of DNA damage [28,29]. Analysis of leucocytes migration to the peritoneum after nanoparticles injection showed an increase in neutrophils and a decrease in lymphocyte levels of D-AMB 5x-treated mice (Fig. 2D). However, similar percentages of neutrophils, leucocytes and monocytes were found between the other treatments. The

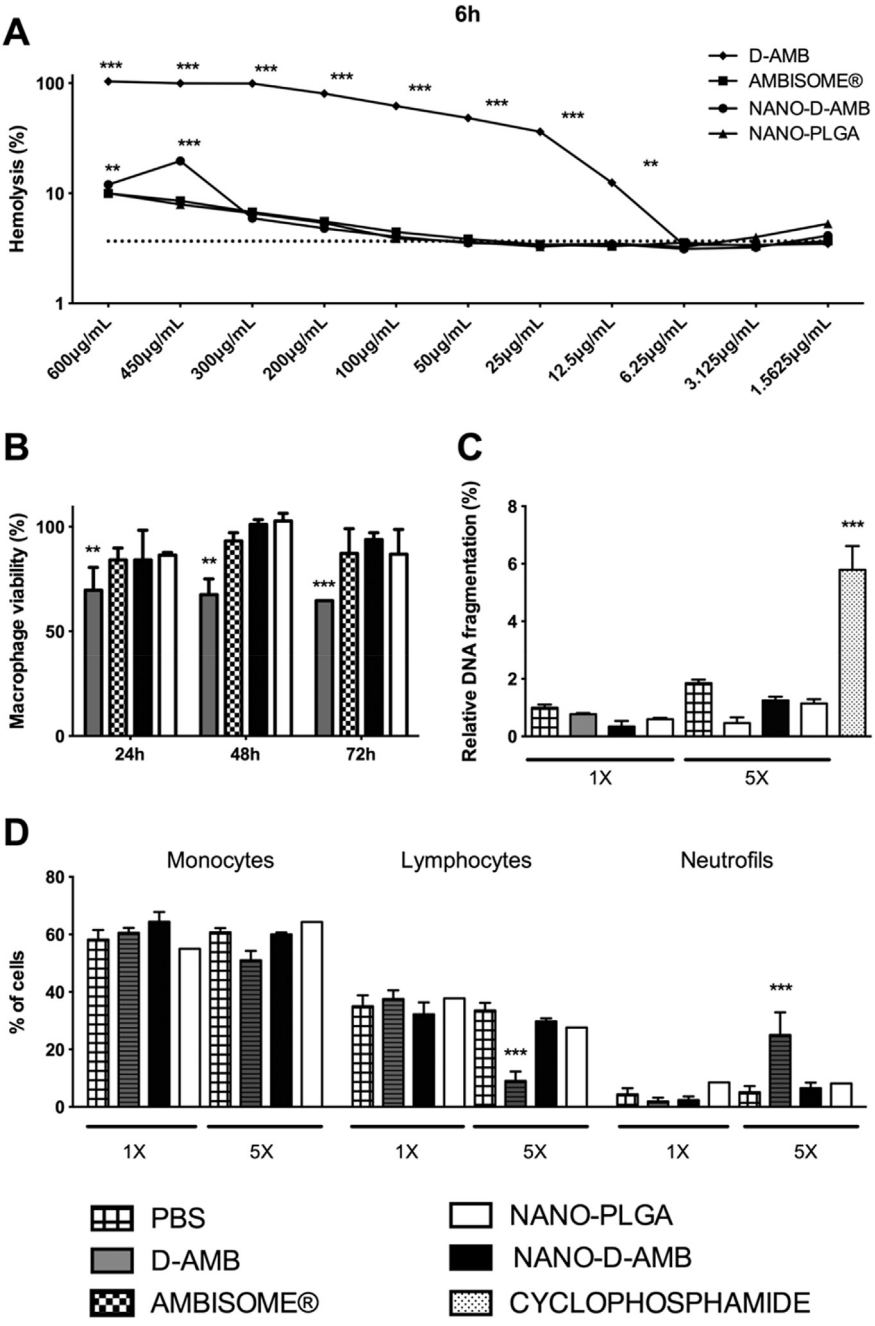

Fig. 2. *In vitro* and *in vivo* safety of NANO-D-AMB. NANO-D-AMB is less hemolytic than D-AMB (A) and does not decrease peritoneal macrophage viability (B) *in vitro*. Dot line represents PBS-treated cells levels of hemolysis (A). *In vivo* toxicity analysis demonstrated that these nanoparticles do not induce genotoxicity in bone-marrow cells (C) or a difference in peritoneal inflammatory cells percentage even upon overdoses (D). The results were expressed as the mean ± SEM. $^{**}p < 0.01$ and $^{***}p < 0.001$ versus PBS treatment.

Table 2
Urea, Creatinine, Uric Acid, AST and ALT levels in healthy animals 3 days after treatment with D-AMB, NANO-D-AMB and NANO-PLGA at indicated doses.

	Urea (mg/dL)	Creatinine (mg/dL)	Uric acid (mg/dL)	AST (U/L)	ALT (U/L)
PBS 1x	69.13 ± 3.16	0.43 ± 0.03	2.75 ± 0.14	97.25 ± 13.63	15.14 ± 3.15
D-AMB 1x	71.22 ± 5.52	0.41 ± 0.01	2.57 ± 0.19	111.00 ± 17.41	20.43 ± 12.28
NANO-D-AMB 1x	66.33 ± 4.163	0.37 ± 0.02	2.64 ± 0.19	98.56 ± 8.39	27.44 ± 8.15
NANO-PLGA 1x	62.56 ± 7.20	0.44 ± 0.04	2.52 ± 0.24	84.89 ± 14.06	23.33 ± 4.33
PBS 5x	54.89 ± 3.32	0.43 ± 0.01	2.35 ± 0.12	86.56 ± 7.68	22.44 ± 0.81
D-AMB 5x	55.56 ± 1.84	0.50 ± 0.02	2.50 ± 0.14	83.22 ± 7.69	22.22 ± 2.13
NANO-D-AMB 5x	68.13 ± 4.17	0.38 ± 0.01	2.54 ± 0.16	82.63 ± 5.30	23.75 ± 2.10
NANO-PLGA 5x	58.40 ± 2.15	0.38 ± 0.02	1.62 ± 0.12**	58.80 ± 6.56	12.20 ± 1.98

The results were expressed as the mean ± SEM. **p < 0.01 compared to PBS 1x group.

quantification of serum biochemical parameters showed a decrease in uric acid in the NANO-PLGA 5X group (Table 2), whereas no changes were observed for the other parameters analyzed. All these data support greater safety in using AMBISOME® and NANO-D-AMB rather than D-AMB.

3.4. Pharmacokinetics parameters

The treatment with NANO-D-AMB resulted in higher plasma concentrations of Amphotericin B at 24 h, 48 h, and 72 h compared with treatment with Anforicin B® (Supplemental Table 1, Fig. 3A). However, pulmonary levels of Amphotericin B were not different at 24 h, 48 h, and 72 h after treatment with NANO-D-AMB or Anforicin B® (Supplemental Table 1, Fig. 3B). Significant difference between the plasma and lung concentrations was observed 24 h after treatment with NANO-D-AMB, when the concentrations of Amphotericin B in the lungs were higher than those obtained from plasma. As for the group treated with Anforicin B®, a significant difference between plasma and lung concentrations of the drug was observed at 24 h and 48 h after treatment. No significant differences were observed in plasma or lung concentrations of Amphotericin B at 24 h, 48 h or 72 h after treatment with NANO-D-AMB or Anforicin B®.

3.5. Biodistribution of 99mTc-labeled nanoparticles

The biodistribution analysis of 99mTc-labeled nanoparticles revealed a higher uptake of 99mTc-NANO-D-AMB nanoparticles in the lungs, liver and spleen when compared to 99mTc-DMSA (Fig. 4A and B). Eight hours after the injection, 99mTc-NANO-D-AMB levels in the lungs were approximately twice as high as 99mTc-DMSA levels. In the liver, 99mTc-NANO-D-AMB levels were about three times more elevated than the 99mTc-DMSA levels (Fig. 4B). Comparing 1 h and 8 h after the injection, serum levels of 99mTc-NANO-D-AMB decreased while tissue levels increased, except for kidneys. The uptake of 99mTc-NANO-D-AMB was lower in the kidneys compared to 99mTc-DMSA at all times investigated (Fig. 4A and B). 99mTc-NANO-D-AMB uptake in kidneys was approximately half of the amount injected of that observed for 99mTc-DMSA 8 h after the injection (Fig. 4B).

The scintigraphic images obtained after administration of 99mTc-DMSA showed the characteristic profile of this radioisotope in which it is mainly uptaken by the urinary system (kidneys and bladder) (Fig. 4C). In contrast, a different pattern was observed for 99mTc-NANO-D-AMB, in which the accumulation was observed in the region of the liver and spleen (Fig. 4C).

3.6. In vivo antifungal therapy using NANO-D-AMB in a paracoccidioidomycosis murine model

Pulmonary fungal load assessed by colony forming units (CFU) quantification showed a significant and similar reduction in groups treated with D-AMB and NANO-D-AMB doses of 6 mg/kg/3days and 4.5 mg/kg/3days (Fig. 5A). The NANO-D-AMB dose of 3 mg/kg/3days was capable of reducing fungal burden significantly compared to the mock-treated group, although it did not reach the same effectiveness of D-AMB or NANO-D-AMB in other doses (Fig. 5A). Treatment with NANO-PLGA led to a similar fungal load of mock-treated group (data not shown). Furthermore, it was observed that both treatments with 6 mg/kg/3days of liposomal Amphotericin B or NANO-D-AMB were similarly able to reduce the fungal load in the lungs (Fig. 5B).

In this experiment, histological analysis (Supplementary Fig. 1) demonstrated presence of numerous granulomatous lesions with yeast cells inside of them in non-treated animals, suggesting the persistence of the pathogen in the tissue, while these were not observed in the groups treated with NANO-D-AMB and AMBISOME®.

In the lymphoproliferation assay, upon stimulation with Concanavalin-A (nonspecific mitogen) and protein extract of *P. brasiliensis* (antigen-specific response), a considerable decrease was observed in the proliferative capacity of splenocytes in all

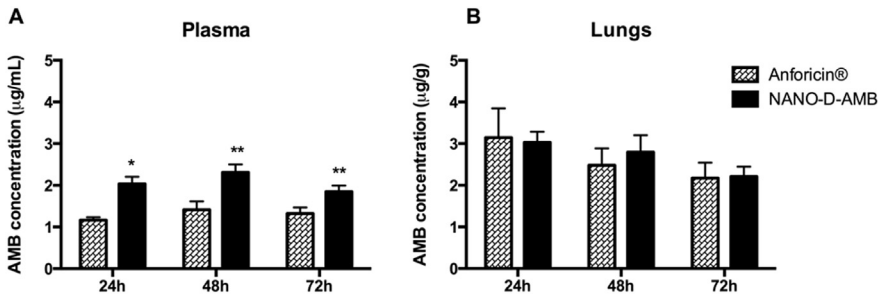

Fig. 3. Plasmatic and lung Amphotericin B concentrations after 24 h, 48 h and 72 h of treatment. Amphotericin B plasmatic concentration in Anforicin B® and NANO-D-AMB treated animals. Plasmatic levels of Amphotericin B were higher after NANO-D-AMB treatment than with Anforicin B® (A). Amphotericin B lung concentration in Anforicin B® and NANO-D-AMB treatment groups (B). The results were expressed as the mean ± SEM. *p < 0.01 and **p < 0.05 to NANO-D-AMB versus Anforicin B® treatment groups.

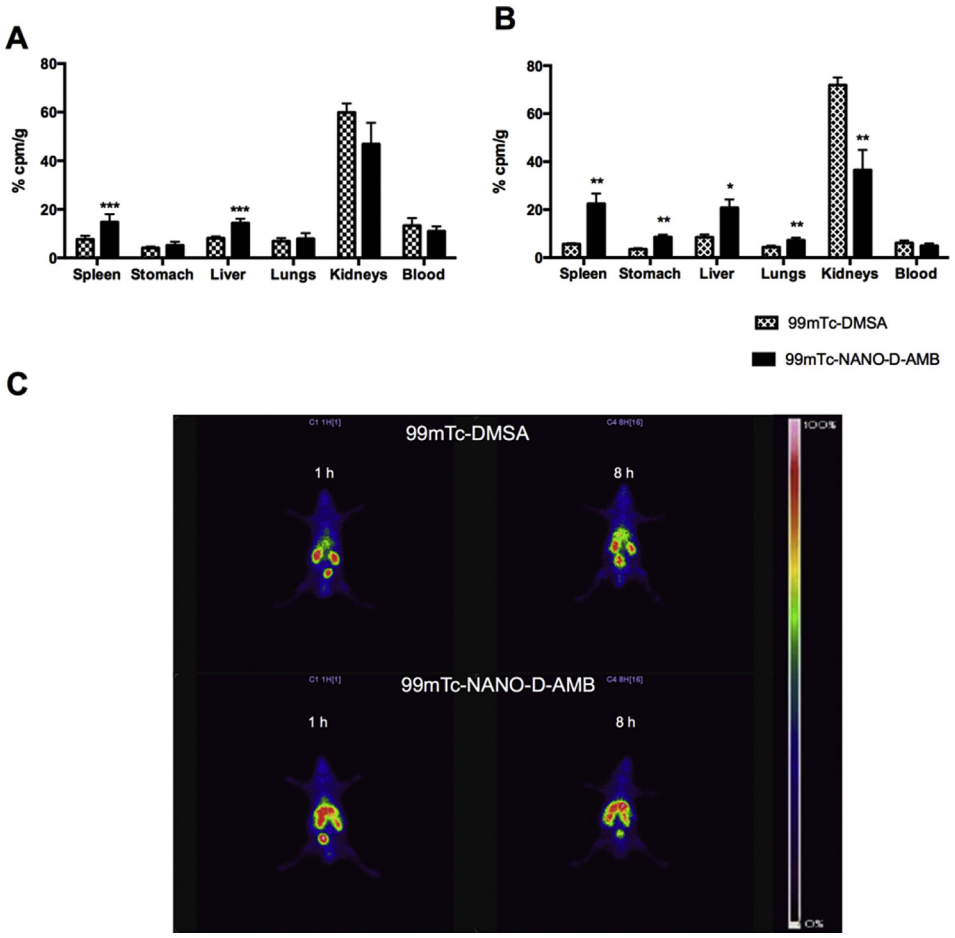

Fig. 4. Biodistribution pattern of nanoparticles labeled with the radioisotope Technetium-99m. Biodistribution after 1 h (A) or 8 h (B) of intravenously administration of 99mTc-NANO-D-AMB (black bars) or 99mTc-DMSA (chequered bars) in mice. The results were expressed as the mean ± SEM. *p < 0.05, **p < 0.01, ***p < 0.001 and ****p < 0.0001 versus control (free DMSA). Biodistribution scintigraphic images after 1 h and 8 h of intravenously injection of 99mTc-DMSA or 99mTc-NANO-D-AMB (C).

groups with infected mice (Fig. 5C). However, treatments with AMBISOME® and NANO-D-AMB appeared to recover this function, even partially, compared with mock-infected animals. An increase was also observed in lung levels of IL-12 in NANO-D-AMB treated groups, while there was no difference in TNF-α and IL-10 levels among groups (Fig. 5D).

4. Discussion

The data presented in this study reinforce the findings observed by Amaral et al. [3], in which Amphotericin B encapsulated within PLGA and DMSA nanoparticles (NANO-D-AMB) was used to treat paracoccidioidomycosis, presenting antifungal activity and preventing nephrotoxic effects in mice. In this previous work, *in vivo* assays also showed that NANO-D-AMB was able to reduce the fungal burden in mice lungs at the same levels as D-AMB, with the advantage of allowing a reduction in the number of injections. In the present study, this antifungal effect was observed even when the mice were treated with a lower amount of nanoparticles, representing only 75% (4.5 mg/kg/3days) of the original dose (6 mg/kg/3days) used in Amaral et al. study [3].

AMBISOME® is one of the commercial liposomal formulations to Amphotericin B, but this lipid formulation is expensive, what limits its widespread use [30–32]. Our findings show that NANO-D-AMB had the same ability than AMBISOME® to reduce lung fungal burden in infected mice. Besides that, both NANO-D-AMB and AMBISOME® increased the proliferation capacity of spleenocytes, which is reduced during paracoccidioidomycosis due to a depression in the host cell immunity [33,34]. NANO-D-AMB treatment also induced higher levels of IL-12, a pro-inflammatory cytokine that is known to present a protective activity against fungal infection, suggesting a potential role of the nanoparticles in modulating the immune response for the host benefit. Together, these data suggest NANO-D-AMB as an alternative antifungal therapy.

Scanning and transmission electron microscopy were used to characterize the nanoparticles, which are useful to determine both morphology and size [35–38]. Blank and Amphotericin B loaded nanoparticles have a uniform spherical shape with a variation in size distribution probably due to the formation of aggregates. The size distribution and the polydispersity index (PDI) of the blank nanoparticles and NANO-D-AMB were compatible with an unimodal distribution and low PDI found in other studies [39–41]. The zeta potential, which reflects the load on the particle surface, presented negative values around 15 mV, enough to ensure the physical stability of the system. In the absence of steric mechanisms, the balance of repulsion and attraction forces determines the stability of nanoparticles. High repulsion forces tend to prevent aggregation and nanoparticles with a zeta potential of approximately (±) 30 mV are more stable in suspension [39,42,43].

The *in vitro* release rates of Amphotericin B from NANO-D-AMB nanoparticles were followed over three days. The data obtained are supported by earlier studies using the same methodology with

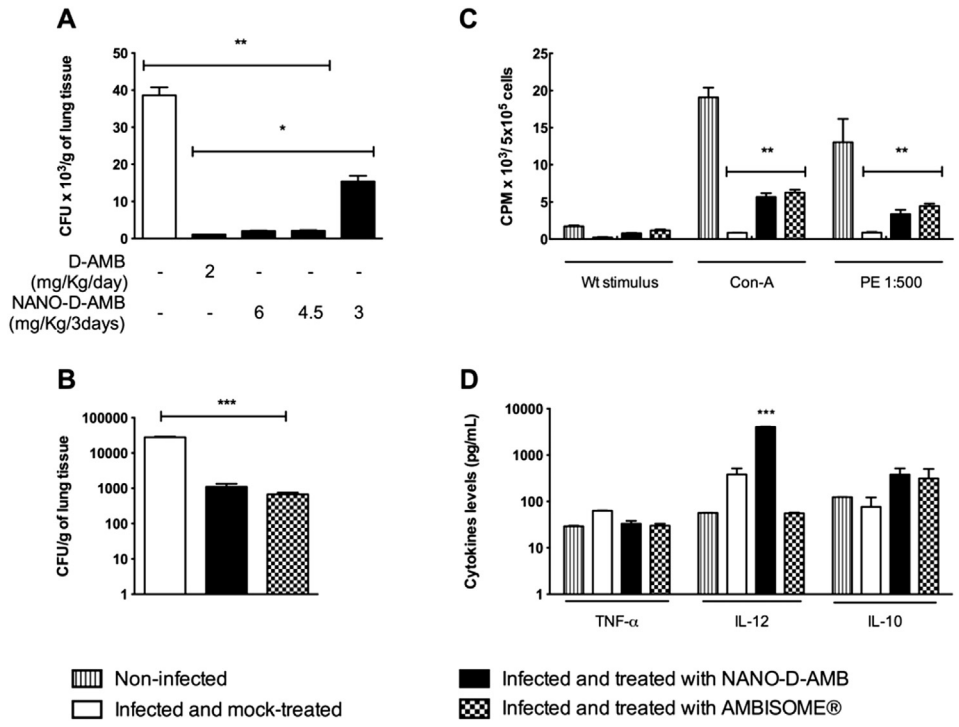

Fig. 5. *In vivo* antifungal therapy using NANO-D-AMB in a paracoccidioidomycosis murine model. NANO-D-AMB treatment reduced fungal burden in the lungs at a comparable level to D-AMB (A) or Ambisome® (B). NANO-D-AMB and Ambisome® therapy increased lymphoproliferation capacity in comparison to non-treated mice in stimulated conditions (C). TNF-α, IL-12 and IL-10 lung levels were assessed by ELISA (D). The results were expressed as the mean ± SEM. *p < 0.05, **p < 0.01 and ***p < 0.001 versus infected and not-treated group.

dialysis membrane and quantification carried out by high-performance liquid chromatography [14]. Corroborating our results, these authors observed a biphasic release characterized by an initial burst, followed by continuous release over 72 h. This release pattern could be explained by a mechanism in which Amphotericin B undergoes diffusion at an earlier moment and then is followed by diffusion and polymer degradation [7]. Probably, the ability for Amphotericin B to dissociate from its carrier is dependent on the solubility of Amphotericin B as well as its concentration.

Pharmacokinetic results showed that the concentration of Amphotericin B in plasma was higher after peritoneal application of NANO-D-AMB than for Anforicin® formulation, indicating a lower drug inactivation. Moreover, it was observed that both Amphotericin B formulations showed similar concentrations in the lungs. However, the concentration of Amphotericin B in NANO-D-AMB-treated animals was slightly higher in the lungs after 48 h and 72 h. Although there were no considerable differences between these formulations, the NANO-D-AMB presented pharmacological advantages since it was injected once every three days, keeping constant levels of the drug in the lung.

The development of systems to deliver drugs to target tissues is receiving great attention in the field of pharmacology and pharmacotherapy. This strategy allows a reduction in the dose required for the therapeutic effect while reducing side effects and toxicity of the drug [44,45]. In our study, DMSA was used as a targeting molecule. DMSA is normally used as a chelating agent against heavy metal intoxication (mainly leads) in doses not higher than 30 mg/kg/day. It accumulates in the kidney, where it is extensively and fast eliminated as a mixed of disulfides of cysteine. In oral treatment, most of the DMSA-cysteine conjugate was eliminated in 24 h [46,47]. In our NANO-D-AMB, DMSA was used as a trace molecule in the final concentration of 0.5 mg/kg/day at the maximum dose of Amphotericin B in our studies (6 mg/kg/day), what is 60 times lower than a normal *in vivo* dose of DMSA used in Lead poisoning. With the purpose of checking a preferential direction of the nanoparticles to specific organs, especially the lungs, the biodistribution of PLGA nanoparticles containing Amphotericin B and DMSA radiolabeled with Technetium-99m was evaluated. This radioisotope is widely used in biodistribution studies of encapsulated drugs [41]. In our experiments, we observed a higher uptake of 99mTc-NANO-D-AMB nanoparticles by the spleen, lungs and liver. These results are in accordance with the scintigraphic images in which we observed the presence of nanoparticles mainly in liver and spleen. Moreover, we hypothesized that because of the addition of DMSA in the nanoparticles, a preferential tropism for the lungs was observed, since a tropism of this molecule for these organs was earlier observed [3]. It is interesting to note the presence of a high amount of 99mTc-NANO-D-AMB in the spleen and lung suggesting that NANO-AMB is a viable therapeutic option because it can accumulate in organs that are normally affected by systemic fungal infections.

In clinical practice 99mTc-DMSA is commonly used for studies of the renal parenchyma as it is secreted and reabsorbed by the renal tubule cells, consistent with the profile image showing the presence of the radioisotope in kidneys and bladder [48,49]. In contrast, the findings indicated that the uptake of 99mTc-NANO-D-AMB was lower in kidneys, almost half of the amount injected. Some studies demonstrated that biodistribution of PLGA nanoparticles without DMSA provided little uptake in the lungs. These differences could be explained partly by the modified surface of nanoparticles with hydrophilic molecules of DMSA, minimizing the opsonization, prolonging the circulation time in blood and eventually decreasing the accumulation of nanoparticles in the liver [50]. Thus, there could be greater retention in the lungs, perhaps due to the presence of blood capillaries of smaller diameter.

One of the most important issues about Amphotericin B clinical

use is the occurrence of side effects, especially nephrotoxicity. Our work demonstrates that the association of Amphotericin B with nanoparticles reduced its presence in the kidneys eight hours after the injection. This fact is relevant as it is expected to reduce the undesirable side effects caused by this drug. Although the amount of Amphotericin B loaded in the nanoparticles was three times higher than the correspondent dose using D-AMB, no adverse effects were identified in lungs, liver and kidney *in vivo*, even upon overdoses, as it is shown by histopathology analysis and quantification of serum biochemical parameters. No genotoxicity in bone marrow cells was identified in mice treated with both blank and Amphotericin B loaded nanoparticles. *In vitro* assays also indicates better biosafety of NANO-D-AMB, since unlike D-AMB treatment, nanoparticles did not induce hemolysis nor macrophages decrease in viability. Besides that, NANO-D-AMB treatment increased the lymphoproliferation and IL-12 levels, which is a very advantageous effect, since it improves the host immune response, increasing the fungal killing and decreasing the chances for a disease relapse.

Together these results demonstrate an alternative approach in the use of Amphotericin B for the treatment of fungal infections. From now on, future studies must be carried out to evaluate NANO-D-AMB efficacy against other fungal and protozoan agents.

Conflict of interest

There is no conflict of interest.

Acknowledgments

The authors wish to thank CNPq (Conselho Nacional de Desenvolvimento Científico e Tecnológico) (554349/2008-6 e 559157/2008-8) and FINEP (Financiadora de Estudos e Projetos) for their financial support. The authors also thank the Laboratory of Clinical Analysis from the University Hospital of Brasília (Brasília/DF).

Appendix A. Supplementary data

Supplementary data related to this article can be found at http://dx.doi.org/10.1016/j.ejmech.2015.03.022.

References

[1] R. Laniado-Laborín, M.N. Cabrales-Vargas, Amphotericin B: side effects and toxicity, Rev. Iberoam. Micol. 26 (2009) 223–227.
[2] D. Ellis, Amphotericin B: spectrum and resistance, J. Antimicrob. Chemother. 49 (Suppl. 1) (2002) 7–10.
[3] A.C. Amaral, A.L. Bocca, A.M. Ribeiro, et al., Amphotericin B in poly(lactic-co-glycolic acid) (PLGA) and dimercaptosuccinic acid (DMSA) nanoparticles against paracoccidioidomycosis, J. Antimicrob. Chemother. 63 (2009) 526–533.
[4] J. Khandare, T. Minko, Polymer–drug conjugates: progress in polymeric prodrugs, Prog. Polym. Sci. 31 (2006) 359–397.
[5] S.A. Costa Lima, M. Resende, R. Silvestre, et al., Characterization and evaluation of BNIPDaoct-loaded PLGA nanoparticles for visceral leishmaniasis: in vitro and in vivo studies, Nanomedicine (Lond) (2012), http://dx.doi.org/10.2217/nnm.12.74.
[6] J.L. Italia, A. Sharp, K.C. Carter, et al., Peroral amphotericin B polymer nanoparticles lead to comparable or superior in vivo antifungal activity to that of intravenous Ambisome® or Fungizone™, PLoS One (October 2011) http://dx.doi.org/10.1371/journal.pone.0025744.
[7] J.L. Italia, M.M. Yahya, D. Singh, M.N. Ravi Kumar, Biodegradable nanoparticles improve oral bioavailability of amphotericin B and show reduced nephrotoxicity compared to intravenous Fungizone, Pharm. Res. 26 (2009) 1324–1331.
[8] K.K. Jain, Applications of nanobiotechnology in clinical diagnostics, Clin. Chem. 2009 (2009) 2002–2009.
[9] Ven H. Van De, C. Paulussen, P.B. Feijens, et al., PLGA nanoparticles and nanosuspensions with amphotericin B: potent in vitro and in vivo alternatives to Fungizone and AmBisome, J. Control Release 161 (2012) 795–803.
[10] R.K. Verma, S. Pandya, A. Misra, Loading and release of amphotericin-B from biodegradable poly(lactic-co-glycolic acid) nanoparticles, J. Biomed. Nanotechnol. 7 (2011) 118–120.
[11] A.L. Bocca, A.C. Amaral, M.M. Teixeira, et al., Paracoccidioidomycosis: eco-epidemiology, taxonomy and clinical and therapeutic issues, Future Microbiol. 8 (2013) 1177–1191.
[12] M.S. Ferreira, Paracoccidioidomycosis, Paediatr. Respir. Rev. 10 (2009) 161–165.
[13] M.P. Garcia, R. Miranda Parca, S. Braun Chaves, et al., Morphological analysis of mouse lungs after treatment with magnetite-based magnetic fluid stabilized with DMSA, J. Magn. Magn. Mater. 293 (2005) 277–282.
[14] M. Nahar, D. Mishra, V. Dubey, N.K. Jain, Development, characterization, and toxicity evaluation of amphotericin B-loaded gelatin nanoparticles, Nanomedicine 4 (2008) 252–261.
[15] A.E. Milner, A.T. Vaughan, I.P. Clark, Measurement of DNA damage in mammalian cells using flow cytometry, Radiat. Res. 110 (1987) 108–117.
[16] P. Blondin, M. Dufour, M a Sirard, Analysis of atresia in bovine follicles using different methods: flow cytometry, enzyme-linked immunosorbent assay, and classic histology, Biol. Reprod. 54 (1996) 631–637.
[17] G.G. Granich, G.S. Kobayashi, D.J. Krogstadl, Sensitive high-pressure liquid chromatographic assay for amphotericin B which incorporates an internal standard. Sensitive high-pressure liquid chromatographic assay for amphotericin b which incorporates an internal standard, Microbiology (1986), http://dx.doi.org/10.1128/AAC..Updated.
[18] L.H. Wang, P.C. Smith, K.L. Anderson, R.M. Fielding, High-performance liquid chromatographic analysis of amphotericin B in plasma, blood, urine and tissues for pharmacokinetic and tissue distribution studies, J. Chromatogr. 579 (1992) 259–268.
[19] I. Echevarría, C. Barturen, M.J. Renedo, M.C. Dios-Viéitez, High-performance liquid chromatographic determination of amphotericin B in plasma and tissue. Application to pharmacokinetic and tissue distribution studies in rats, J. Chromatogr. A 819 (1998) 171–176.
[20] P.O. Gubbins, B.J. Gurley, J. Bowman, Rapid and sensitive high performance liquid chromatographic method for the determination of itraconazole and its hydroxy-metabolite in human serum, J. Pharm. Biomed. Anal. 16 (1998) 1005–1012.
[21] I. Echevarría, C. Barturen, M.J. Renedo, et al., Comparative pharmacokinetics, tissue distributions, and effects on renal function of novel polymeric formulations of amphotericin B and amphotericin B-deoxycholate in rats, Antimicrob. Agents Chemother. 44 (2000) 898–904.
[22] I. Bekersky, R.M. Fielding, D.E. Dressler, et al., Pharmacokinetics, excretion, and mass balance of liposomal amphotericin B (AmBisome) and amphotericin B deoxycholate in humans, Antimicrob. Agents Chemother. 46 (2002) 828–833.
[23] E. Tessier, L. Neirinck, Z. Zhu, High-performance liquid chromatographic mass spectrometric method for the determination of ursodeoxycholic acid and its glycine and taurine conjugates in human plasma, J. Chromatogr. B Anal. Technol. Biomed. Life Sci. 798 (2003) 295–302.
[24] H. Vogelsinger, S. Weiler, A. Djanani, et al., Amphotericin B tissue distribution in autopsy material after treatment with liposomal amphotericin B and amphotericin B colloidal dispersion, J. Antimicrob. Chemother. 57 (2006) 1153–1160.
[25] A.F. Marques, M.B. da Silva, M.A. Juliano, et al., Additive effect of P10 immunization and chemotherapy in anergic mice challenged intratracheally with virulent yeasts of Paracoccidioides brasiliensis, Microbes Infect. 10 (2008) 1251–1258.
[26] M.D. Berliner, M.E. Reca, Vital staining of Histoplasma capsulatum with Janus Green B, Med. Mycol. 5 (1967) 26–29.
[27] T. Ehrenfreund-Kleinman, T. Azzam, R. Falk, et al., Synthesis and characterization of novel water soluble amphotericin B-arabinogalactan conjugates, Biomaterials 23 (2002) 1327–1335.
[28] N. Chernoff, J.M. Rogers, A.J. Alles, et al., Cell cycle alterations and cell death in cyclophosphamide teratogenesis, Teratog. Carcinog. Mutagen 9 (1989) 199–209.
[29] D. Anderson, J.B. Bishop, R.C. Garner, et al., Cyclophosphamide: review of its mutagenicity for an assessment of potential germ cell risks, Mutat. Res. 330 (1995) 115–181.
[30] A. Gullo, Invasive fungal infections: the challenge continues, Drugs 69 (Suppl. 1) (2009) 65–73.
[31] Pauw B. De, Antifungal therapy, TPS 43 (2011) 2461–2462.
[32] S.J. Thornton, K.M. Wasan, The reformulation of amphotericin B for oral administration to treat systemic fungal infections and visceral leishmaniasis, Expert Opin. Drug Deliv. 6 (2009) 271–284.
[33] A.M. Ribeiro, A.L. Bocca, A.C. Amaral, et al., HSP65 DNA as therapeutic strategy to treat experimental paracoccidioidomycosis, Vaccine 28 (2010) 1528–1534.
[34] A.M. Ribeiro, A.L. Bocca, A.C. Amaral, et al., DNAhsp65 vaccination induces protection in mice against Paracoccidioides brasiliensis infection, Vaccine 27 (2009) 606–613.
[35] H.J. Jeon, Y.I. Jeong, M.K. Jang, et al., Effect of solvent on the preparation of surfactant-free poly(DL-lactide-co-glycolide) nanoparticles and norfloxacin release characteristics, Int. J. Pharm. 207 (2000) 99–108.
[36] M.-H. Kim, J. Lee, S.-Y. Mo, et al., Synthesis and characterization of silver nanoparticle composite with poly(p-Br-phenylsilane), J. Nanosci. Nanotechnol. 12 (2012) 4344–4347.
[37] R. Romano-Trujillo, E. Rosendo, M. Ortega, et al., Synthesis and characterization of PbSe nanoparticles obtained by a colloidal route using Extran as a surfactant at low temperature, Nanotechnology 23 (2012) 185602.
[38] S. Vilayurganapathy, A. Devaraj, R. Colby, et al., Subsurface synthesis and

characterization of Ag nanoparticles embedded in MgO, Nanotechnology 24 (2013) 095707.
[39] R. Fernández-Urrusuno, P. Calvo, C. Remuñán-López, et al., Enhancement of nasal absorption of insulin using chitosan nanoparticles, Pharm. Res. 16 (1999) 1576–1581.
[40] T. Govender, S. Stolnik, M.C. Garnett, et al., PLGA nanoparticles prepared by nanoprecipitation: drug loading and release studies of a water soluble drug, J. Control Release 57 (1999) 171–185.
[41] K. Avgoustakis, Pegylated poly(lactide) and poly(lactide-co-glycolide) nanoparticles: preparation, properties and possible applications in drug delivery, Curr. Drug Deliv. 1 (2004) 321–333.
[42] S.R. Schaffazick, S.S. Guterres, L. de L. Freitas, A.R. Pohlmann, Caracterização e estabilidade físico-química de sistemas poliméricos nanoparticulados para administração de fármacos, Quim Nova 26 (2003) 726–737.
[43] V.J. Mohanraj, Y. Chen, Nanoparticles – a review, Trop. J. Pharm. Res. 5 (2006) 561–573.
[44] M. Kleinberg, What is the current and future status of conventional amphotericin B? Int. J. Antimicrob. Agents 27 (Suppl. 1) (2006) 12–16.
[45] M. Nahar, T. Dutta, S. Murugesan, et al., Functional polymeric nanoparticles: an efficient and promising tool for active delivery of bioactives, Crit. Rev. Ther. Drug Carr. Syst. 23 (2006) 259–318.
[46] R.B. Azevedo, C.R.A. Valois, S.B. Chaves, et al., Leukocyte transepithelial migration in lung induced by DMSA functionalized magnetic nanoparticles, Cell. Adhes. Migr. 5 (2011) 29–33.
[47] S. Bradberry, T. Sheehan, A. Vale, Use of oral dimercaptosuccinic acid (succimer) in adult patients with inorganic lead poisoning, Qjm 102 (2009) 721–732.
[48] Mda C. Lopes de Lima, C.D. Ramos, S.Q. Brunetto, et al., Estimation of absolute renal uptake with technetium-99m dimercaptosuccinic acid: direct comparison with the radioactivity of nephrectomy specimens, Sao Paulo Med. J. 126 (2008) 150–155.
[49] K. Avgoustakis, A. Beletsi, Z. Panagi, et al., Effect of copolymer composition on the physicochemical characteristics, in vitro stability, and biodistribution of PLGA-mPEG nanoparticles, Int. J. Pharm. 259 (2003) 115–127.
[50] B. Semete, L. Booysen, Y. Lemmer, et al., In vivo evaluation of the biodistribution and safety of PLGA nanoparticles as drug delivery systems, Nanomedicine 6 (2010) 662–671.